Integrative Medicine Research 13 (2024) 101051

Contents lists available at ScienceDirect

Integrative Medicine Research

journal homepage: www.elsevier.com/locate/imr

Original Article

Peripheral Rho-associated protein kinase activation mediates acupuncture analgesia

Ji-Yeun Park [a], Jae-Hwan Jang [b], Yang-Hwa Kang [c], Songhee Jeon [d], Seung-Nam Kim [e], Yeon-Hee Ryu [f], Hi-Joon Park [c,*]

[a] College of Korean Medicine, Daejeon University, Daejeon, Republic of Korea
[b] Jaseng Spine and Joint Research Institute, Jaseng Medical Foundation, Seoul, Republic of Korea
[c] Studies of Translational Acupuncture Research, Acupuncture and Meridian Science Research Center, Kyung Hee University, Seoul, Republic of Korea
[d] Department of Biomedical Sciences, Center for Creative Biomedical Scientists at Chonnam National University, Gwangju, Republic of Korea
[e] College of Korean Medicine, Dongguk University, Goyang, Republic of Korea
[f] KM Science Research Division, Korea Institute of Oriental Medicine, Daejeon, Republic of Korea

ARTICLE INFO

Keywords:
Acupuncture
Analgesia
Rho associated protein kinase
Peripheral
Molecular mechanism

ABSTRACT

Background: Acupuncture has been proven effective for various types of pain, and peripheral molecular signals around acupuncture-treated areas have been suggested to contribute to the analgesic effects of acupuncture. However, the underlying mechanism from these peripheral molecular signals to central ones remains unclear. The purpose of this study was to investigate whether peripheral Rho-associated protein kinase (ROCK) activation induced by acupuncture treatment mediates acupuncture analgesia, and also to investigate the relationship between ROCK activation and extracellular signal-regulated kinase (ERK), which has previously been proven to mediate acupuncture analgesia and other related molecular changes during acupuncture.

Methods: Acupuncture was treated at the bilateral GB34 acupoints of C57BL/6 mice, after which changes in ROCK activation and the location of its expression in the skin were analyzed. To verify the role of ROCK in acupuncture analgesia, we administrated ROCK inhibitor Y-27632 (0.3 μg/ul) into the skin before acupuncture treatment with formalin and complete Freund adjuvant (CFA) induced pain models, then the nociceptive responses were analyzed.

Results: Acupuncture treatment produced ROCK2 activation in the skin after 30 and 60 min, and the histological analyses revealed that ROCK2 was activated in the fibroblast of the dermis. The acupuncture-induced ROCK2 expression was significantly attenuated by the ERK inhibitor, whereas phospho-ERK expression was not inhibited by ROCK inhibitor. In both the formalin- and CFA-induced mouse pain models, acupuncture analgesia was blocked by ROCK inhibitor administration.

Conclusion: Acupuncture treatment-induced ROCK2 expression is a downstream effector of phospho-ERK in the skin and plays a crucial role in acupuncture analgesia.

1. Introduction

Acupuncture is a non-pharmacological treatment that has been proven effective for various types of pain.[1–3] Despite the clinical effectiveness of acupuncture analgesia, understanding of the mechanisms of its action is still not comprehensive.

A 'central mechanism' is known to be involved in acupuncture analgesia, which entails a descending inhibitory pathway, endogenous central and spinal opioids, and glial deactivation in the spinal cord.[4,5] Peripheral changes following acupuncture treatments are also indicated to mediate the analgesic effect. Abraham et al. and Wu et al. have reported that the transient receptor potential vanilloid 1 (TRPV1) is expressed after acupuncture treatment at the stimulated site, which is related to acupuncture analgesia.[6,7] Burnstock hypothesized the involvement of purinergic signaling in analgesic mechanisms of acupuncture and proposed that acupuncture-induced ATP release in keratinocytes, fibroblasts, and other cells in the skin could send impulses through sensory nerve endings to the brain that inhibit the neural pathways of pain sensation.[8] Goldman et al. also indicated the importance of adenine nucleotides (i.e., adenosine, adenosine monophosphate (AMP), adenosine diphosphate (ADP), and adenosine triphosphate (ATP)) released by acupuncture treatment; the adenosine A1 receptor is necessary for the

* Corresponding author at: Studies of Translational Acupuncture Research, Acupuncture and Meridian Science Research Center, Kyung Hee University, 26 Kyungheedae-ro, Dongdaemoon-gu, Seoul 02447, Republic of Korea.
E-mail address: acufind@khu.ac.kr (H.-J. Park).

https://doi.org/10.1016/j.imr.2024.101051
Received 19 September 2023; Received in revised form 29 May 2024; Accepted 30 May 2024
Available online 31 May 2024

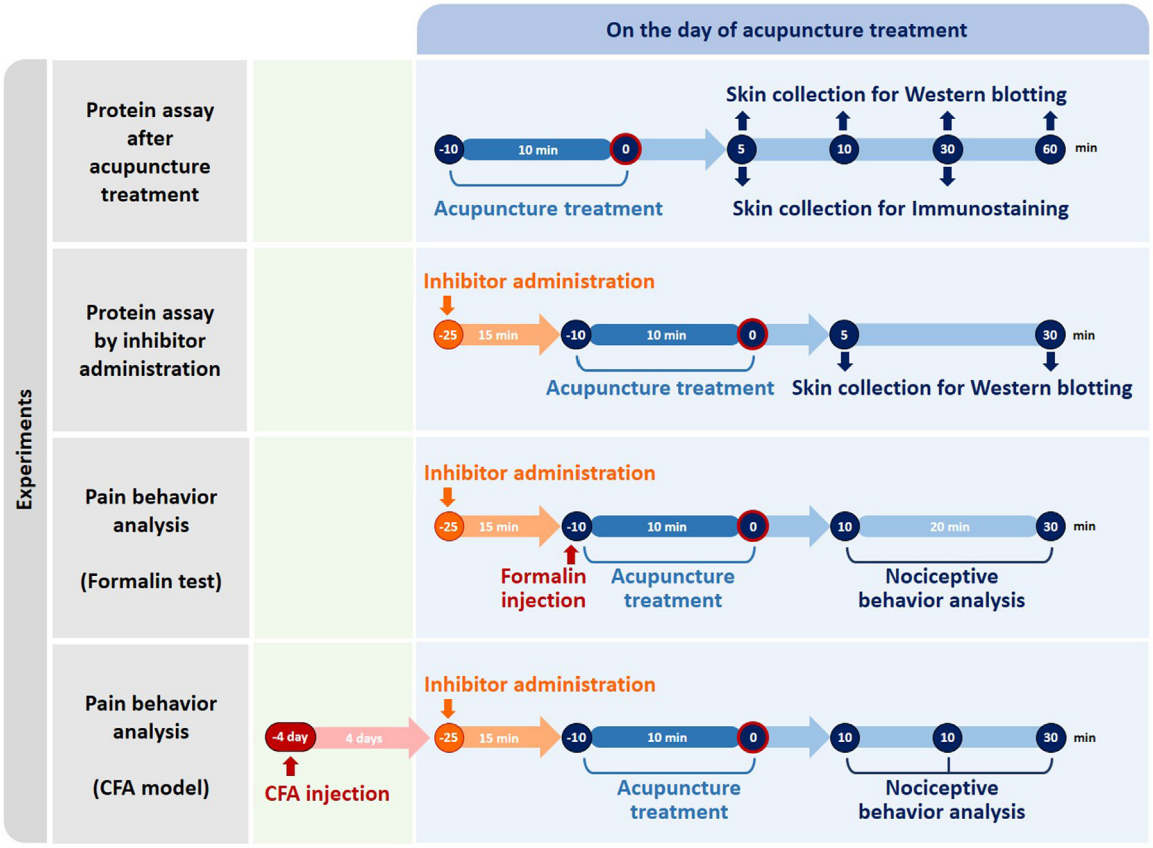

Fig. 1. Experimental schedule of this study. CFA, complete Freund adjuvant.

local antinociceptive action of acupuncture analgesia.[9,10] Nitric oxide-cGMP, a catalyzing enzyme, activation and changes of skin impedance also have been identified as acupuncture-induced factors.[11,12]

Our previous studies[13,14] found that acupuncture treatment activated extracellular signal-regulated kinase (pERK) in the skin, leading to acupuncture analgesia. Morphological changes induced by acupuncture treatment in the fibroblasts of subcutaneous loose connective tissue are known to remodel the cytoskeleton and may be an important factor in the effect of acupuncture. Previously, Langevin et al. demonstrated that Rho-associated protein kinase (ROCK) is necessary for the cytoskeletal remodeling induced by acupuncture manipulation.[15,16] However, the relationship between ROCK activation and the therapeutic effects of acupuncture remain untested. Thus, we investigated whether acupuncture-induced tissue deformation activates ROCK expression in the skin layer and mediates acupuncture analgesia. Additionally, we explored the relationship between ERK activation and other related molecular changes during acupuncture in the skin.

2. Methods

2.1. Animals

Male C57BL/6 mice (at 8–9 weeks of age, weighing 20–25 g) were purchased from Samtaco, Inc. (Seoul, Korea). Mice were maintained on a 12 /12 hour (h) light/dark schedule with free access to food and water. All the experiments were approved by the Kyung Hee University Animal Care Committee for animal welfare [KHUASP(SE)-13-053-1] and were performed according to the guidelines of the NIH and the Korean Academy of Medical Sciences and followed the recommendations of the International Association for the Study of Pain (IASP). All experimental schedules are shown in Fig. 1.

2.2. Drug administration

Bilateral leg hair was removed using an electronic hair clipper (Voguers, Bucheon-si, Gyeonggi-Do, Korea) before the experiment. On the day of the experiment, mice were lightly anesthetized with ether, and 10 μl of U0126 (ERK inhibitor, 0.8 ug/ul in dimethyl sulfoxide (DMSO); Promega, Madison, WI, USA),[17–19] or Y-27632 (ROCK inhibitor, 0.3 ug/ul in distilled water; Sigma, St. Louis, MO, USA)[15,16] was intradermally injected into the GB34 acupuncture point using 0.5 ml syringes (BD Biosciences, San Jose, CA, USA) 15 minutes (min) before acupuncture treatment to inhibit molecular activation.[20] Control mice were injected equal volume of vehicle.

2.3. Acupuncture treatment

On the day of the experiment, mice were immobilized in a holder, and then acupuncture needles (0.18 mm in diameter and 8 mm in length; Haenglim-seoweon Acuneedle Co., Yeoju-gun, Kyonggi-do, Republic of Korea) were inserted to a depth of 3 mm at the bilateral GB34 (*Yangneungcheon*) acupuncture point. On the fibular aspect of the leg, GB34 is located in the depression anterior and distal to the head of the fibula,[21] and GB34 has been known to have an effect on pain and motor dysfunction.[13,22,23] Acupuncture needles were rotated at a rate of two spins per second bidirectional of 180° for 10 s (s) and removed 10 min later. The depth of insertion and the rate of rotation for the acupuncture-needling technique were verified using Acusensor (Acupuncture needling force and motion sensor system; Stromatec, Inc., Burlington, VT, USA).[24]

2.4. Skin sample collection

After removing the acupuncture needles, mice were anesthetized with ether, and the acupuncture-treated skin tissues (5 mm in diame-

ter, above the muscle) were collected 5, 10, 30, or 60 min later. For the control, the same part of the skin tissues from the control mice was collected using the same methods. For western blotting, skin tissues were immediately put into liquid nitrogen, then stored at -80°C. For immunostaining, skin tissues were immediately put into 4 % formalin solution for fixation.

2.5. Western blot analyses

Skin samples were pulverized in liquid nitrogen and were homogenized in 200 μl of lysis buffer (Invitrogen, Carlsbad, CA, USA), with phosphatase inhibitor cocktail tablets (Roche, Indianapolis, IN, USA) and protease inhibitor cocktail tablets (Roche) in distilled water. After homogenization, the samples were centrifuged at 12,000 rpm for 15 min at 4°C and the supernatants were then collected. Protein concentrations were determined using the bicinchoninic acid (BCA) assay. For Western blot analyses, equal protein concentrations (i.e., 10 μg of total protein) were separated by 8–10 % sodium dodecyl sulfate-polyacrylamide gel electrophoresis (SDS-PAGE), after which they were transferred to a polyvinylidene fluoride (PVDF) membrane (Amersham Biosciences, Buckinghamshire, UK). This membrane was blocked in 5 % skim milk in Tris buffered saline containing 0.1 % Tween-20 (TBS-T) and was incubated with primary antibodies overnight at 4°C — these primary antibodies were rabbit phosphorylated extracellular signal-regulated kinase (p-ERK), total ERK, ROCK1, ROCK2, phosphorylated ezrin-radixin-moesin (p-ERM), ERM (Cell Signaling Technology, Beverly, MA, USA), and mouse β-actin (Sigma). The PVDF membrane was also incubated with secondary horseradish peroxidase-conjugated goat anti-rabbit antibodies (Pierce, Rockford, IL, USA) and goat anti-mouse antibodies (Pierce). The membrane was visualized using a chemiluminescence kit (Super Signal West Pico; Pierce) and signal intensities from the immunoblots were quantified using an Image Quant TL (GE Healthcare, Uppsala, Sweden).

2.6. Immunohistochemistry

A few days after fixation, all skin samples were embedded in paraffin, then cut into 4 μm slices and placed on microscope slides. To remove the paraffin, the sections were incubated in xylene and were then hydrated in 100 % ethanol and 95 % ethanol; sections were also washed in distilled H_2O. For immunohistochemistry analyses, all sections were incubated in 3 % hydrogen peroxide for 10 min, washed in wash buffer (TBS-T), and were incubated in blocking solution (i.e., TBS-T with 5 % BSA) for 1 h. The blocking solution was removed and the primary rabbit ROCK2 antibody (Novus Biologicals, Littleton, CO, USA) was diluted in the blocking solution and were added to each section; these solutions were incubated overnight at 4°C. Then, the antibody solution was removed, and the sections were rinsed with wash buffer. The sections were incubated with biotinylated anti-rabbit immunoglobulin G (IgG; Vector Laboratories Inc, Burlingame, CA, USA) for 1 h. All sections were then incubated with the avidin-biotin-peroxidase complex (ABC) reagent (Vector Laboratories Inc.) and were incubated in 0.02 % diaminobenzidine, 0.003 % hydrogen peroxide, and 1 M Tris-buffered saline (pH 7.5). As soon as the sections were developed, all slides were immersed in distilled H_2O. The sections then were counterstained with hematoxylin, dehydrated in 95 % and 100 % ethanol, incubated in xylene, and were mounted. Images of the layers of the skin were taken using a bright-field microscope (BX51; Olympus, Tokyo, Japan).

2.7. Immunofluorescence

For immunofluorescence analyses, all sections were washed in a wash buffer and then incubated in blocking solution for 1 h. The blocking solution was removed and the primary antibodies of ROCK2 (Novus Biologicals) and mouse fibroblasts (5B5; Abcam, Cambridge, United Kingdom) were diluted in the blocking solution and were added to the sections; these solutions were incubated overnight at 4°C. The antibody solution was removed and sections were washed with the wash buffer. The sections were then incubated using Alexa Fluor 488 anti-mouse IgG (Invitrogen) and Alexa Fluor 594 anti-rabbit IgG (Invitrogen) for 1 h in a dark room and were mounted using mounting medium with 40,6-diamidino-2-phenylindole (DAPI; Vector Laboratories Inc.). The ROCK2 and 5B5 positive signals were detected using confocal microscopy (FV10i; Olympus).

2.8. Formalin-induced mouse pain model and behavior assessment

All mice were divided into five groups: injected with formalin (FOR), injected with formalin and Y-27632 (FOR+Y), injected with formalin and treated with acupuncture (ACU), injected with formalin and Y-27632, and treated with acupuncture (ACU+Y), and treated with control procedures (CON; $n = 6$ in each group).

On the day of the experiment, all the mice were acclimatized in a clear acrylic chamber (20 cm in diameter and height) for 30 min before the experiment. Mice in the FOR+Y and ACU+Y groups were intradermally injected with Y-27632 at bilateral GB34. Mice of the CON, FOR, and ACU groups were injected with equal volumes of distilled water (i.e., 10 μl) at GB34 15 min before the acupuncture treatment, as a control for Y-27632. Fifteen min later, Mice in the FOR, FOR+Y, ACU, and ACU+Y groups were all injected with 1 % formalin (20 μl, diluted in saline) into the plantar surface of the right hind paw subcutaneously, as previously described.[25,26] Equal volumes of saline (i.e., 20 μl) was injected into the right hind paw of the mice in the CON group as a control for the formalin injection. Mice of ACU and ACU+Y groups were treated with acupuncture at bilateral GB34 right after formalin injection then immobilized for 10 min. Mice of the CON, FOR, and FOR+Y groups were also immobilized for 10 min to cause an equal amount of stress.

To assess nociceptive behavior, mice were immediately placed back into the same acrylic chamber after acupuncture treatment. Then, the nociceptive responses were recorded using a video camera from 10 to 30 min after the formalin injection. The total time spent flinching, licking, and biting the right hind paw was measured and analyzed during each 5-min block.

2.9. CFA-induced mouse pain model and behavior assessment

All mice were divided into five groups: injected with complete Freund's adjuvant (CFA) only (CFA), injected with CFA and Y-27632 (CFA+Y), injected with CFA and treated with acupuncture (ACU), injected with CFA and Y-27632, and treated with acupuncture (ACU+Y), and treated with control procedures (CON; $n = 6$ in each group).

All the mice were habituated in a clear acryl box (8 cm x 10 cm x 10 cm, with a gridded floor) for 1 h daily for 2 d. Next day, after 1 h habituation using same method, the mechanical threshold of the bilateral hind paws under baseline conditions was assessed using electronic von Frey filaments (IITC, Woodland Hills, CA, US). A von Frey filament exerting 0.6 g of force was applied 10 times to the plantar surface of each hind paw, for 1 s at a time with 5 s intervals. The frequency of the positive responses from a total of the 10 trials was calculated for each foot. Four days later, mice of the CFA, CFA+Y, ACU, and ACU+Y groups were injected with 100 μl of CFA emulsion solution (CFA; suspended in oil and mixed with an equal volume of saline) into the plantar surface of the right hind paw subcutaneously, as previously described.[27] Equal volumes of saline (i.e., 100 μl) were injected into the right hind paw of the CON group mice as a control for CFA injection. After CFA injection, the mechanical threshold was assessed to confirm nociceptive behaviors of pain. Then, mice of the CFA+Y and ACU+Y groups were injected with 3 μg/10 μl Y-27632 at bilateral GB34. Mice in the CON, CFA, and ACU groups were injected with equal volumes of distilled water (i.e., 10 μl) at bilateral GB34 as a control for Y-27632. Fifteen minutes later, mice of the ACU and ACU+Y groups were treated with acupuncture at bilateral GB34 then immobilized for 10 min. The mice of the CON, CFA,

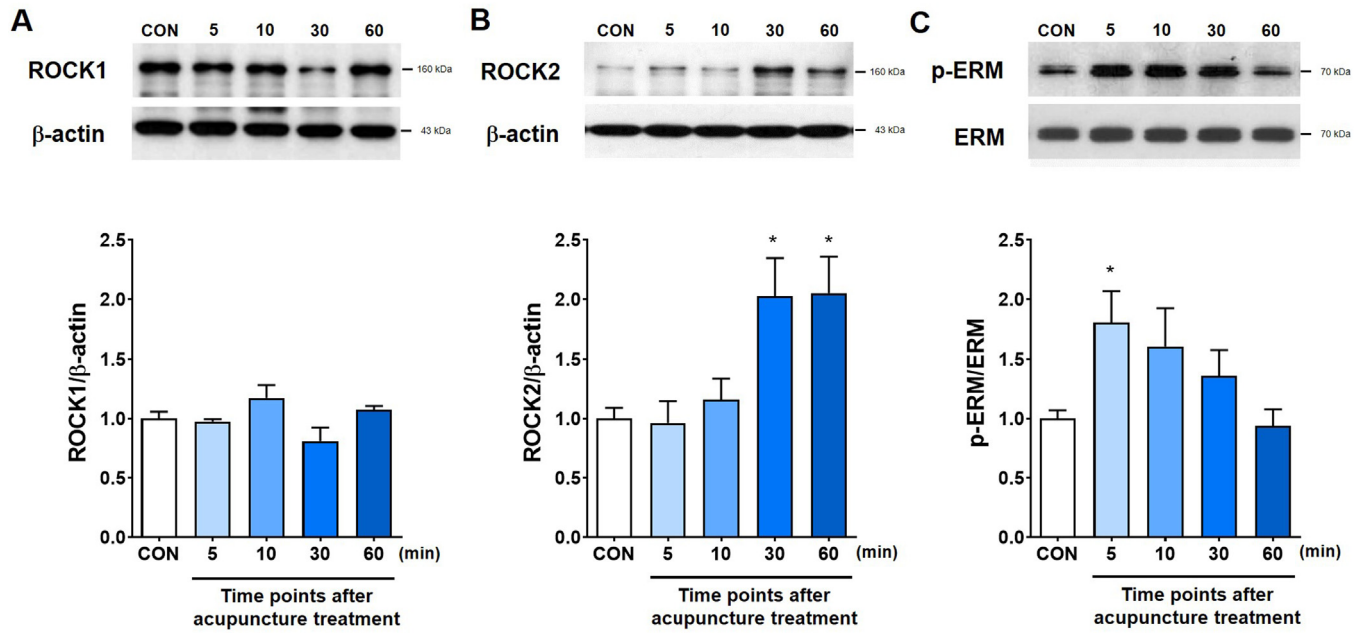

Fig. 2. ROCK1, ROCK2, and p-ERM expression in the skin after acupuncture treatment. Expression levels of (A) ROCK1, (B) ROCK2, and (C) p-ERM in the skin were determined at 5, 10, 30, and 60 min after acupuncture treatment via western blotting analyses. ROCK2 activation increased significantly at 30 and 60 min after acupuncture treatment compared to that in the control group (B). Activation of p-ERM was increased significantly 5 min after acupuncture treatment (C). Here, $^{*}p < 0.05$ compared to the CON group followed by the Student's *t*-test (each $n = 3$–5) and error bars indicate the SEM. CON, treated with no acupuncture; ROCK, Rho-associated protein kinase; p-ERM, phosphorylated ezrin-radixin-moesin.

and CFA+Y groups were also immobilized for 10 min to cause an equal amount of stress as the acupuncture treated groups. After acupuncture needing, all mice were immediately placed back into the same clear box and the mechanical threshold of the bilateral hind paws was assessed.

2.10. Statistical analysis

The GraphPad Prism 9 software (GraphPad Software Inc., San Diego, CA, USA) was used for all statistical analyses. All data were expressed as the mean ± standard error of the mean (SEM). Statistical analyses were performed using unpaired Student's *t*-test, one-way ANOVA with the Newman–Keuls post-hoc test, and two-way ANOVA followed by a Bonferroni post-hoc test. In all of the aforementioned analyses, the differences were considered statistically significant at $p < 0.05$.

3. Results

3.1. ROCK1, ROCK2, and p-ERM expression in the skin after acupuncture treatment

To investigate protein changes related to tissue deformation after acupuncture treatment, the expression levels of ROCK1, ROCK2, and p-ERM in the skin were determined 5, 10, 30, and 60 min after acupuncture treatment, respectively. After acupuncture treatment, ROCK2 increased significantly at 30 and 60 min after acupuncture treatment compared to that in the control group ($p < 0.05$), while the activation of p-ERM increased significantly 5 min after acupuncture treatment ($p < 0.05$; Fig. 2A–C).

3.2. ROCK2 activation in the skin after acupuncture

Immunostainings were performed to verify the expression location of ROCK2. In the immunohistochemistry analysis, ROCK2 was activated in the fibroblasts of dermis after acupuncture treatment ($p < 0.01$; Fig. 3A). To verify the cell type of ROCK2 activation, skin tissues were stained with 5B5, a fibroblast marker, and were then visualized for immunofluorescence. It was confirmed that the cells where ROCK2 was activated via acupuncture treatment were fibroblasts, since they were co-stained with a fibroblast marker (Fig. 3B).

3.3. Inhibition of acupuncture induced ROCK2, p-ERK, and p-ERM activation by U0126 and Y-27632

We investigated the correlation between localized ERK activation and tissue deformation-related molecules such as ROCK2 and ERM using U0126. Acupuncture-induced ROCK2 and p-ERM expression was significantly attenuated by U0126 administration ($p < 0.01$; Fig. 3C-D). ROCK2 activation in the skin was successfully inhibited by the Y-27632 administration (Fig. 3E). Acupuncture induced p-ERK expression was attenuated by U0126, but not by Y-27632 administration. Acupuncture induced p-ERM expression was attenuated by U0126 and Y-27632 administration (Fig. 3F). This implies that ERK acts in the early part of the acupuncture-induce local molecular signaling pathway, as well as the fact that ROCK2 and p-ERM act as downstream effectors of ERK activation after acupuncture.

3.4. ROCK activation in the skin mediates acupuncture analgesia in formalin-induced acute mouse pain model

To verify whether acupuncture-induced localized ROCK activation mediates acupuncture analgesia, we administered Y-27632 in the formalin-induced and CFA induced mouse pain models. In the formalin-induced mouse pain model, nociceptive responses of the FOR group were more significantly increased than that in the CON group ($p < 0.001$). FOR+Y group showed the same degree of nociceptive response as the FOR group ($p < 0.001$ vs. CON), suggesting that the administration of Y-27632 into the skin did not affect the nociceptive response to formalin. Acupuncture treatment significantly attenuated the nociceptive responses when compared to that in the FOR group ($p < 0.001$) and that acupuncture analgesia was diminished by Y-27632 administration ($p < 0.01$; Fig. 4A). The analgesic effects of acupuncture

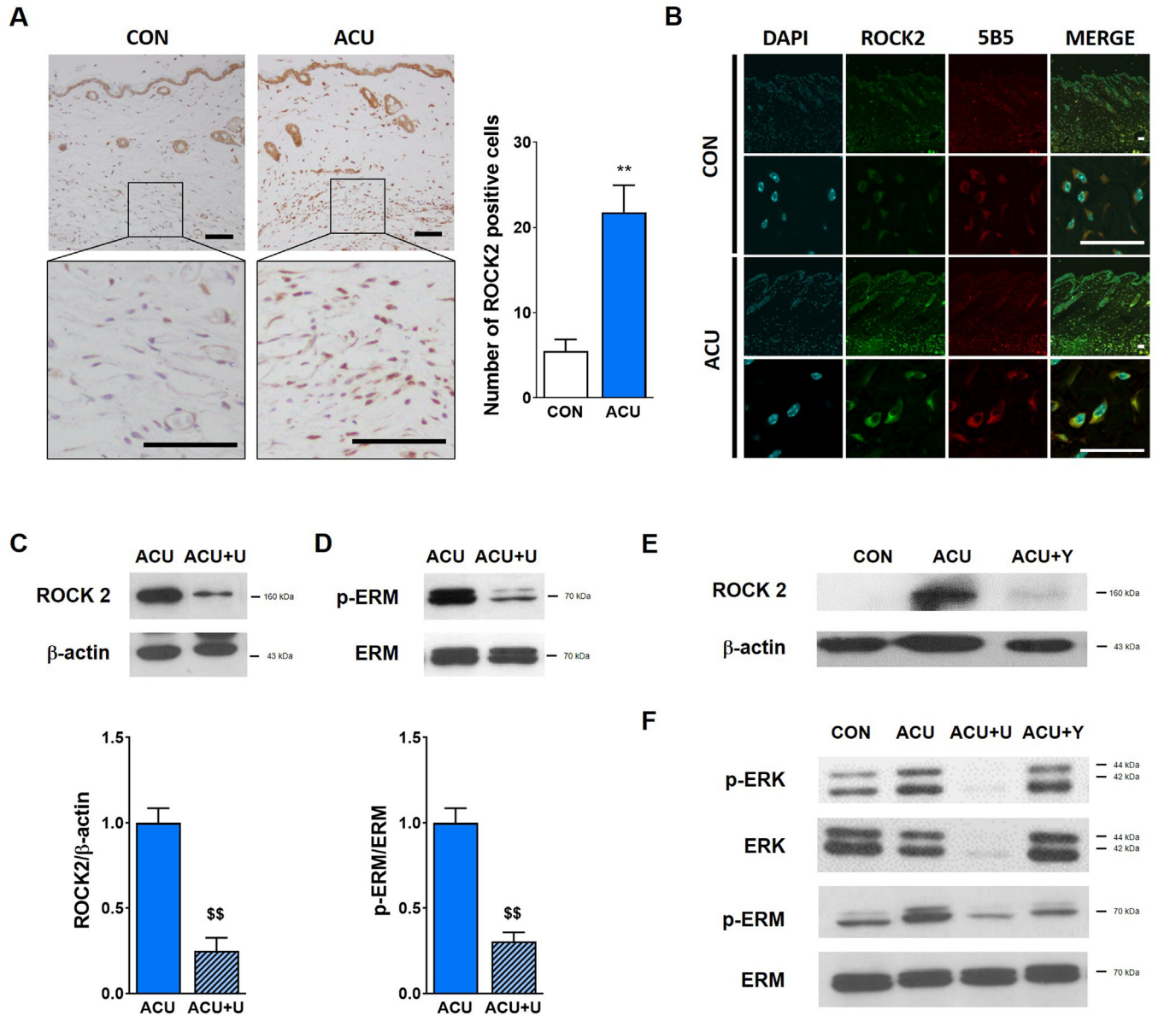

Fig. 3. ROCK2 expression in the skin after acupuncture treatment, and inhibition of acupuncture-induced ROCK2, p-ERM, and p-ERK activation by U0126 (i.e., ERK inhibitor) and Y-27632 (i.e., ROCK inhibitor). (A-B) ROCK2 was activated in the skin, especially in the fibroblasts of the dermis 30 min after acupuncture treatment. 5B5, fibroblast marker. Blue: counterstain with 40,6-diamidino-2-phenylindole (DAPI), Green: expression of ROCK2, Red: expression of 5B5, a fibroblast marker. (C-D) Acupuncture induced ROCK2 and p-ERM activation was attenuated by U0126 administration, injected at the GB34 acupuncture point intradermally. (E) Acupuncture-induced ROCK2 activation in the skin was significantly attenuated by 0.3 μg/ul of Y-27632. (F) Acupuncture induced p-ERK expression was attenuated by U0126, but not by Y-27632 administration. Acupuncture induced p-ERM expression was attenuated by U0126 and Y-27632 administration. Scale bar: 100 μm (A) and 20 μm (B). $^{**}p < 0.01$ compared to the CON group; $^{\$\$}p < 0.01$ compared to the ACU group followed by the Student's *t*-test (each $n = 3$). Error bars indicate the SEM. ACU, treated with acupuncture; ACU+U, treated with U0126 and acupuncture; ACU+Y, treated with Y-27632 and acupuncture; CON, treated with no acupuncture; p-ERK, phosphorylated extracellular signal-regulated kinase; p-ERM, phosphorylated ezrin-radixin-moesin; ROCK, Rho-associated protein kinase.

and the inhibitory effect of Y-27632 on it were most remarkable at approximately 25–30 min after the acupuncture treatment (Fig. 4B).

3.5. ROCK activation in the skin mediates acupuncture analgesia in CFA-induced sub-chronic mouse pain model

In the CFA-induced sub-chronic mouse pain model, the mechanical pain threshold of the right hind paw was significantly more increased after CFA injection compared to that of the CON group ($p < 0.001$); that of CFA+Y group was as same as CFA group ($p < 0.001$ vs. CON). Mice in the ACU group showed a significant decrease in pain behavior than that of the CFA group from 10–30 min ($p < 0.001$). Acupuncture analgesia was blocked by Y-27632 ($p < 0.001$; Fig. 4C). The contralateral side, i.e., the left hind paw, did not show significant differences between the CFA and ACU groups (Fig. 4D).

4. Discussion

In this study, we found that ROCK2 was activated following ERK activation via acupuncture-induced molecular changes and acupuncture analgesia was blocked by the ROCK inhibitor Y-27632. These results suggest that ROCK2 activation, resulting from the cytoskeletal deformation induced by acupuncture treatment, is an important factor in producing the analgesic effects of acupuncture. To the best of our

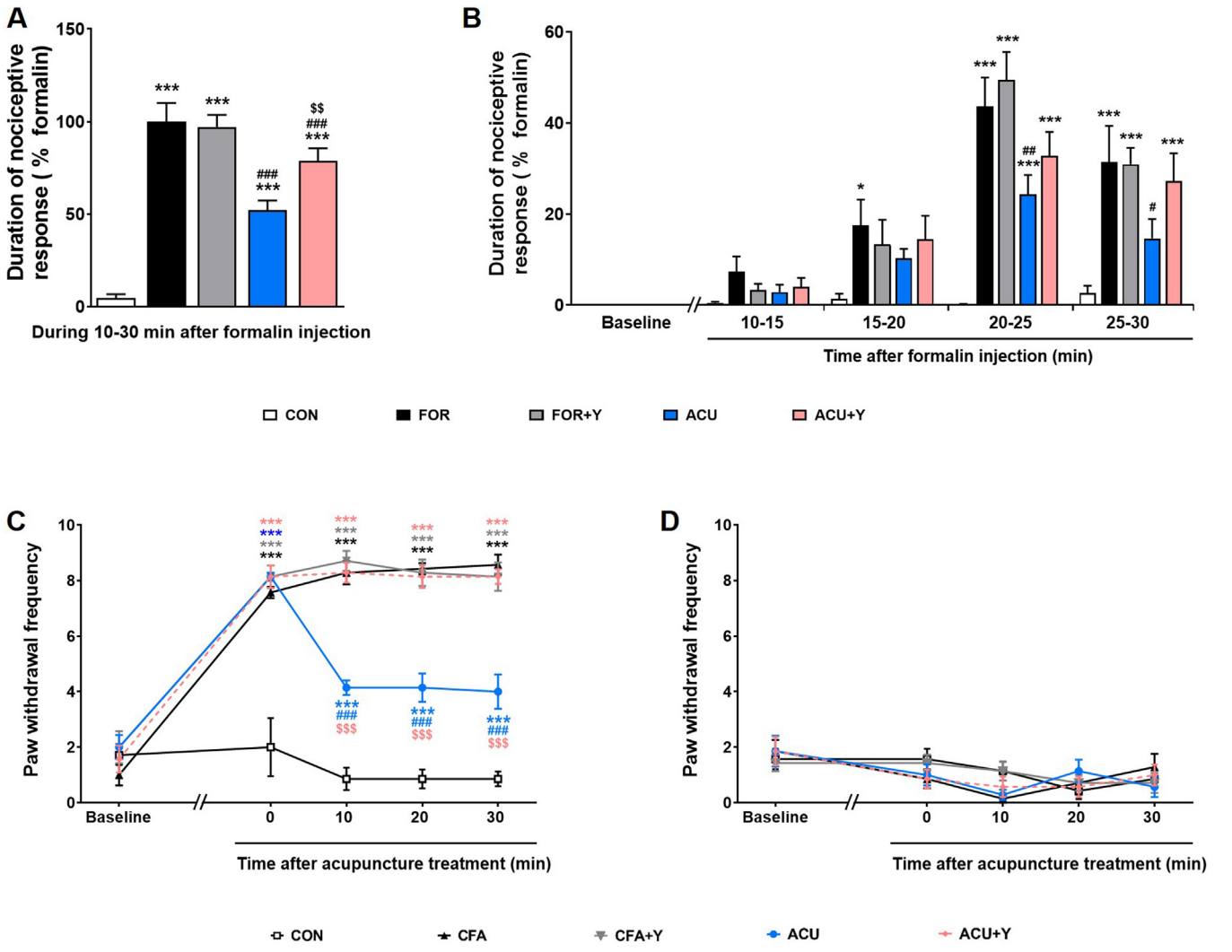

Fig. 4. The analgesic effects of acupuncture treatment were reversed by Y-27632 administration in mouse pain models induced by formalin and complete Freund's adjuvant (CFA). (A-B) The duration of the formalin-evoked nociceptive response, such as flinching, licking, and biting of the right hind paw, was analyzed during 10-30 min after the formalin injection (A) and during each 5-minute block (B). (C-D) The frequency of positive responses was determined using a von Frey filament exerting 0.6 g of force (C: ipsilateral, D: contralateral) every 10 min after acupuncture treatment in a CFA-induced mouse pain model. $^{*}p < 0.05$ and $^{***}p < 0.001$ compared to the CON group; $^{\#}p < 0.05$, $^{\#\#}p < 0.01$, and $^{\#\#\#}p < 0.001$ compared to the FOR or CFA group; $^{\$\$}p < 0.01$, $^{\$\$\$}p < 0.001$ compared to the ACU group. One-way ANOVA was followed by the Newman–Keuls test (A) and 2-way ANOVA was followed by the Bonferroni test (B-D) (A-B: each $n = 8$, C-D: each $n = 7$). Error bars indicate SEM. ACU, injected with formalin or CFA, and treated with acupuncture; ACU+Y, injected with formalin or CFA, administered Y-27632, and treated with acupuncture; CFA, injected with CFA; CFA+Y, injected with CFA and administered Y-27632. CON, treated with control procedures; FOR, injected with formalin; FOR+Y, injected with formalin and administered Y-27632.

knowledge, this is the first study to investigate cytoskeletal responses around the acupuncture point in relation to the analgesic effects of acupuncture.

Mechanical tissue deformation around the acupuncture point is the first physiological phenomenon after acupuncture treatment. It has been suggested that cytoskeletal remodeling in response to tissue deformation induced by acupuncture needle manipulation contributes to an important process in understanding acupuncture mechanism.[27–29] Langevin et al. reported that fibroblasts of skin tissues around the needle point were deformed by acupuncture manipulation, resulting in the activation of various downstream cascades.[28] These cascades contribute in mediating the clinical effect of acupuncture; moreover, the Rho/Rac kinase signaling is one of the possible cascades that is involved in the cytoskeletal remodeling process of fibroblasts during acupuncture.[15,16] ROCK, which are serine/threonine kinases, are involved in many aspects of cell motility such as cell migration, proliferation, gene expression, actin cytoskeleton, and/or microtubule network, and other common cellular functions.[30] Two ROCK isoforms, ROCK1 and ROCK2, have 65 % overall identity of amino acid sequences and 92 % homology within their kinase domains. Although the common cellular activity of ROCK1 and ROCK2 is regulating actomyosin cytoskeleton, they have a distinct role in regulating actin cytoskeleton reorganization and cell detachment. It has been reported that ROCK1 is involved in destabilizing the actin cytoskeleton through peripheral actomyosin contraction, whereas ROCK2 is required for stabilizing the actin cytoskeleton.[31–34] In our results, only ROCK2 was activated after acupuncture treatment, whereas ROCK1 showed no significant change. These results suggest that ROCK2 may be involved in the rearrangement of local skin tissue that is damaged by mechanical stimulation via needles. In addition, the analgesic effect of acupuncture was significantly blocked by Y-27632, suggesting that ROCK2 expression after acupuncture is a major factor mediating the analgesic effect of acupuncture.

The ROCK protein has numerous downstream effectors such as ERM, adducin and MLC, and is also related to ERK signaling.[7,35–37] Since

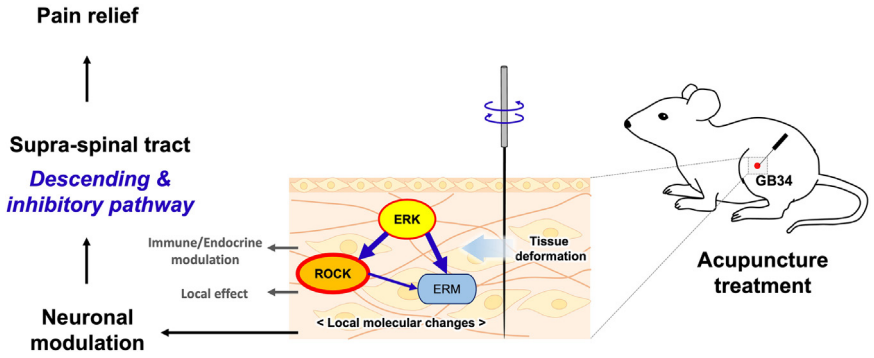

Fig. 5. Hypothesis of signaling transduction mechanism of acupuncture analgesia from peripheral molecular responses to central analgesic pathway. Acupuncture was performed at the GB34 acupuncture point. In the local molecular changes, ERK was activated as a trigger molecule that activates ERM and ROCK proteins and the activated ROCK was strongly involved with acupuncture analgesia. Localized molecular signaling might be connected to the descending inhibitory pathway of supra-spinal tract, resulting in overall pain relief. Displacement, a linear movement of the needle; ERK, extracellular signal–regulated kinase; ERM, ezrin-radixin-moesin; Rev, revolution; ROCK, rho-associated protein kinase.

ROCK is one of the main molecules that is activated by cytoskeletal remodeling of fibroblast, peripheral cascade activation by acupuncture treatment contributes to mediating acupuncture analgesia. Moreover, we investigated the correlation between ROCK and other molecules which were previously reported to influence the effect of acupuncture. ERK was one of the critical molecules contributing to acupuncture analgesia based on our previous work[13,14] and ERM was a downstream effector of the Rho/Rac protein. Our results indicated that ERK activation participates in initiating the signaling pathway and acts as a trigger molecule that initiates the acupuncture-induced local molecular signaling pathway. The ROCK2 activation following ERK activation contributes to the analgesic mechanism of acupuncture. These signaling occur around the acupuncture point and is involved in the peripheral mechanisms of acupuncture.

Pain is mediated by neural activity through the central and peripheral nervous system. Accordingly, therapeutic approaches including acupuncture treatment involve regulating both top-down (i.e., central neural pathways) and bottom-up (i.e., peripheral neural pathways) mechanisms.[38,39] We suggest a hypothesis of a signal transduction mechanism of acupuncture analgesia from peripheral molecular responses to central analgesic pathway. Acupuncture treatment produces numerous cascades in the skin; among these, ERK signaling is activated in the initial phase and has a role in inducing other cascades, while ERM and ROCK is activated in the later part of the signaling pathway. These peripheral molecular signals affect the activation of the nervous or vascular system around the acupuncture-treated site. These responses are transmitted through the spinal cord by the sensory afferents of ascending nerve tracts and then transferred to the supra-spinal tract to relieve pain by modulating the descending inhibitory pathway (Fig. 5).[40–47]

In conclusion, we found that ROCK2 is activated prominently in the fibroblasts of the skin, is a downstream effector of pERK during acupuncture-induced molecular changes, and plays a crucial role in mediating acupuncture analgesia. Further studies are still needed to elucidate how these peripheral molecular activities are linked to central mechanism of acupuncture analgesia, such as the opioid system or the descending inhibitory pathways. In addition, comparing various control groups of acupuncture treatment, such as without manipulation, electroacupuncture, and non-acupoint treatment, is necessary to identify the detailed mechanical mechanism of acupuncture treatment in the future.

CRediT authorship contribution statement

Ji-Yeun Park: Conceptualization, Writing – original draft, Funding acquisition, Data curation. **Jae-Hwan Jang:** Validation. **Yang-Hwa Kang:** Writing – original draft, Formal analysis. **Songhee Jeon:** Conceptualization, Methodology. **Seung-Nam Kim:** Conceptualization, Methodology. **Yeon-Hee Ryu:** Conceptualization, Methodology. **Hi-Joon Park:** Conceptualization, Writing – original draft, Funding acquisition, Data curation.

Declaration of competing interest

The authors declare that there are no financial or other relationships that might lead to a conflict of interest.

Funding

This research was supported by grants from the Korea Institute of Oriental Medicine (Grant K18182) and the National Research Foundation of Korea (NRF) grand funded by the Korean government (MSIT) (No. NRF-2021R1A2C2006818, RS-2023-00210098, and RS-2023-00260439).

Ethical statement

All the experiments were approved by the Kyung Hee University Animal Care Committee for animal welfare [KHUASP(SE)-13-053-1].

Data availability

The data will be made available upon request.

Supplementary materials

Supplementary material associated with this article can be found, in the online version, at doi:10.1016/j.imr.2024.101051.

References

1. Vickers AJ, Cronin AM, Maschino AC, et al. Acupuncture for chronic pain: individual patient data meta-analysis. *Arch Intern Med*. 2012;172(19):1444–1453.
2. He Y, Guo X, May BH, et al. Clinical evidence for association of acupuncture and acupressure with improved cancer pain: a systematic review and meta-analysis. *JAMA Oncol*. 2020;6(2):271–278. doi:10.1001/jamaoncol.2019.5233.
3. Lee IS, Cheon S, Park JY. Central and peripheral mechanism of acupuncture analgesia on visceral pain: a systematic review. *Evid Based Complement Alternat Med*. 2019;2019:1304152.
4. Lai HC, Lin YW, Hsieh CL. Acupuncture-analgesia-mediated alleviation of central sensitization. *Evid-Based Complement Alternat Med*. 2019;2019:6173412.
5. Lyu Z, Guo Y, Gong Y, et al. The role of neuroglial crosstalk and synaptic plasticity-mediated central sensitization in acupuncture analgesia. *Neural Plast*. 2021;2021:8881557.
6. Abraham TS, Chen ML, Ma SX. TRPV1 expression in acupuncture points: response to electroacupuncture stimulation. *J Chem Neuroanat*. 2011;41(3):129–136. doi:10.1016/j.jchemneu.2011.01.001.

7. Wu SY, Chen WH, Hsieh CL, Lin YW. Abundant expression and functional participation of TRPV1 at Zusanli acupoint (ST36) in mice: mechanosensitive TRPV1 as an "acupuncture-responding channel. *BMC Complement Alternat Med*. 2014;14(1):96. doi:10.1186/1472-6882-14-96.
8. Burnstock G. Acupuncture: a novel hypothesis for the involvement of purinergic signalling. *Med Hypotheses*. 2009;73(4):470–472.
9. Goldman N, Chen M, Fujita T, et al. Adenosine A1 receptors mediate local anti-nociceptive effects of acupuncture. *Nat Neurosci*. 2010;13(7):883–888. doi:10.1038/nn.2562.
10. Takano T, Chen X, Luo F, et al. Traditional acupuncture triggers a local increase in adenosine in human subjects. *J Pain*. 2012;13(12):1215–1223. doi:10.1016/j.jpain.2012.09.012.
11. Thong T, Colbert AP, Larsen AP. An 8-channel skin impedance measurement system for acupuncture research. *Proceedings of the Annual International Conference of the IEEE Engineering in Medicine and Biology Society* IEEE; 2009:861–864.
12. Jou NT, Ma SX. Responses of nitric oxide–cGMP release in acupuncture point to electroacupuncture in human skin in vivo using dermal microdialysis. *Microcirculation*. 2008;16(5):434–443 Vol 16, No 5. doi:10.1080/10739680902915012.
13. Park JY, Park JJ, Jeon S, et al. From peripheral to central: the role of ERK signaling pathway in acupuncture analgesia. *J Pain*. 2014;15(5):535–549. doi:10.1016/j.jpain.2014.01.498.
14. Park JY, Cho SJ, Lee SH, et al. Peripheral ERK modulates acupuncture-induced brain neural activity and its functional connectivity. *Sci Rep*. 2021;11(1):5128. doi:10.1038/s41598-021-84273-y.
15. Langevin HM, Bouffard NA, Badger GJ, Churchill DL, Howe AK. Subcutaneous tissue fibroblast cytoskeletal remodeling induced by acupuncture: evidence for a mechanotransduction-based mechanism. *J Cell Physiol*. 2006;207(3):767–774. doi:10.1002/jcp.20623.
16. Langevin HM, Bouffard NA, Fox JR, et al. Fibroblast cytoskeletal remodeling contributes to connective tissue tension. *J Cell Physiol*. 2011;226(5):1166–1175. doi:10.1002/jcp.22442.
17. Favata MF, Horiuchi KY, Manos EJ, et al. Identification of a novel inhibitor of mitogen-activated protein kinase kinase. *J Biol Chem*. 1998;273(29):18623–18632. doi:10.1074/jbc.273.29.18623.
18. Davies SP, Reddy H, Caivano M, Cohen P. Specificity and mechanism of action of some commonly used protein kinase inhibitors. *Biochem J*. 2000;351(Pt 1):95–105. doi:10.1042/0264-6021:3510095.
19. Lim JH, Gibbons HM, O'Carroll SJ, Narayan PJ, Faull RLM, Dragunow M. Extracellular signal-regulated kinase involvement in human astrocyte migration. *Brain Res*. 2007;1164:1–13. doi:10.1016/j.brainres.2007.06.020.
20. Dai Y, Iwata K, Fukuoka T, et al. Phosphorylation of extracellular signal-regulated kinase in primary afferent neurons by noxious stimuli and its involvement in peripheral sensitization. *J Neurosci*. 2002;22(17):7737–7745. doi:10.1523/JNEUROSCI.22-17-07737.2002.
21. World Health Organization. *WHO Standard Acupuncture Point Locations in the Western Pacific Region*. WHO Regional Office for the Western Pacific; 2008 Accessed July 24, 2023 *https://apps.who.int/iris/handle/10665/353407* .
22. Sun S, Cao H, Han M, Li TT, Zhao ZQ, Zhang YQ. Evidence for suppression of electroacupuncture on spinal glial activation and behavioral hypersensitivity in a rat model of monoarthritis. *Brain Res Bull*. 2008;75(1):83–93. doi:10.1016/j.brainresbull.2007.07.027.
23. Mi WL, Mao Ying QL, Wang XW, et al. Involvement of spinal neurotrophin-3 in electroacupuncture analgesia and inhibition of spinal glial activation in rat model of monoarthritis. *J Pain*. 2011;12(9):974–984. doi:10.1016/j.jpain.2011.03.002.
24. Davis RT, Churchill DL, Badger GJ, Dunn J, Langevin HM. A new method for quantifying the needling component of acupuncture treatments. *Acupunct Med*. 2012;30(2):113–119. doi:10.1136/acupmed-2011-010111.
25. Randolph BC, Peters MA. Analgesic effectiveness of ketorolac compared to meperidine in the rat formalin test. *Anesth Prog*. 1997;44(1):11–16.
26. Kim HY, Wang J, Lee I, Kim HK, Chung K, Chung JM. Electroacupuncture suppresses capsaicin-induced secondary hyperalgesia through an endogenous spinal opioid mechanism. *Pain*. 2009;145(3):332–340. doi:10.1016/j.pain.2009.06.035.
27. Langevin HM, Churchill DL, Wu J, et al. Evidence of connective tissue involvement in acupuncture. *FASEB J*. 2002;16(8):872–874. doi:10.1096/fj.01-0925fje.
28. Langevin HM, Churchill DL, Cipolla MJ. Mechanical signaling through connective tissue: a mechanism for the therapeutic effect of acupuncture. *FASEB J*. 2001;15(12):2275–2282. doi:10.1096/fj.01-0015hyp.
29. Langevin HM, Bouffard NA, Churchill DL, Badger GJ. Connective tissue fibroblast response to acupuncture: dose-dependent effect of bidirectional needle rotation. *J Altern Complement Med*. 2007;13(3):355–360. doi:10.1089/acm.2007.6351.
30. Riento K, Ridley AJ. ROCKs: multifunctional kinases in cell behaviour. *Nat Rev Mol Cell Biol*. 2003;4(6):446–456. doi:10.1038/nrm1128.
31. Nakagawa O, Fujisawa K, Ishizaki T, Saito Y, Nakao K, Narumiya S. ROCK-I and ROCK-II, two isoforms of Rho-associated coiled-coil forming protein serine/threonine kinase in mice. *FEBS Lett*. 1996;392(2):189–193. doi:10.1016/0014-5793(96)00811-3.
32. Lock FE, Hotchin NA. Distinct roles for ROCK1 and ROCK2 in the regulation of keratinocyte differentiation. *PLoS One*. 2009;4(12):e8190. doi:10.1371/journal.pone.0008190.
33. Shi J, Wu X, Surma M, et al. Distinct roles for ROCK1 and ROCK2 in the regulation of cell detachment. *Cell Death Dis*. 2013;4(2) e483-e483. doi:10.1038/cddis.2013.10.
34. Shi J, Surma M, Zhang L, Wei L. Dissecting the roles of ROCK isoforms in stress-induced cell detachment. *Cell Cycle*. 2013;12(10):1492–1500. doi:10.4161/cc.24699.
35. Amano M, Fukata Y, Kaibuchi K. Regulation and functions of Rho-associated kinase. *Exp Cell Res*. 2000;261(1):44–51. doi:10.1006/excr.2000.5046.
36. Laboureau J, Dubertret L, Lebreton-De Coster C, Coulomb B. ERK activation by mechanical strain is regulated by the small G proteins rac-1 and rhoA. *Exp Dermatol*. 2004;13(2):70–77. doi:10.1111/j.0906-6705.2004.00117.x.
37. Hong SY, Jeon YM, Lee HJ, Kim JG, Baek JA, Lee JC. Activation of RhoA and FAK induces ERK-mediated osteopontin expression in mechanical force-subjected periodontal ligament fibroblasts. *Mol Cell Biochem*. 2010;335(1):263–272. doi:10.1007/s11010-009-0276-1.
38. Kuner R. Central mechanisms of pathological pain. *Nat Med*. 2010;16(11):1258–1266. doi:10.1038/nm.2231.
39. Reidler JS, Mendonca ME, Santana MB, et al. Effects of motor cortex modulation and descending inhibitory systems on pain thresholds in healthy subjects. *J Pain*. 2012;13(5):450–458. doi:10.1016/j.jpain.2012.01.005.
40. Cabioğlu MT, Cetin BE. Acupuncture and immunomodulation. *Am J Chin Med*. 2008;36(1):25–36. doi:10.1142/S0192415X08005552.
41. Hirano T, Zeredo JL, Kimoto M, Moritaka K, Nasution FH, Toda K. Disinhibitory involvement of the anterior cingulate cortex in the descending antinociceptive effect induced by electroacupuncture stimulation in rats. *Am J Chin Med*. 2008;36(03):569–577. doi:10.1142/S0192415X08005989.
42. Zhao ZQ. Neural mechanism underlying acupuncture analgesia. *Prog Neurobiol*. 2008;85(4):355–375. doi:10.1016/j.pneurobio.2008.05.004.
43. Tang JS, Qu CL, Huo FQ. The thalamic nucleus submedius and ventrolateral orbital cortex are involved in nociceptive modulation: a novel pain modulation pathway. *Prog Neurobiol*. 2009;89(4):383–389. doi:10.1016/j.pneurobio.2009.10.002.
44. Guo ZL, Longhurst JC. Activation of reciprocal pathways between arcuate nucleus and ventrolateral periaqueductal gray during electroacupuncture: involvement of VGLUT3. *Brain Res*. 2010;1360:77–88. doi:10.1016/j.brainres.2010.08.102.
45. Chen CY, Chern RS, Liao MH, Chang YH, Hsu JYC, Chien CH. The possible neuronal mechanism of acupuncture: morphological evidence of the neuronal connection between groin A-Shi point and uterus. *Evid Based Complement Alternat Med*. 2013;2013:429186. doi:10.1155/2013/429186.
46. Kim W, Kim SK, Min BI. Mechanisms of electroacupuncture-induced analgesia on neuropathic pain in animal model. *Evid Based Complement Alternat Med*. 2013;2013:e436913. doi:10.1155/2013/436913.
47. Zhang R, Lao L, Ren K, Berman BM. Mechanisms of acupuncture-electroacupuncture on persistent pain. *Anesthesiology*. 2014;120(2):482–503. doi:10.1097/ALN.0000000000000101.